ELSEVIER

Ceramics International 30 (2004) 2023–2027

CERAMICS INTERNATIONAL

www.elsevier.com/locate/ceramint

Soft optical phonon in Ba-doped $Sr_2Nb_2O_7$ ceramics

A. Hushur [a,*], Y. Akishige [b], S. Kojima [a]

[a] *Institute of Materials Science, Tsukuba University, Tsukuba, Ibaraki 305-8573, Japan*
[b] *Faculty of Education, Shimane University, Matsue 690-8504, Japan*

Received 28 November 2003; received in revised form 15 December 2003; accepted 23 December 2003

Available online 2 July 2004

Abstract

The Raman scattering technique was applied to examine the soft optical phonon of the $Ba_{0.32}Sr_{0.68}Nb_2O_7$ in the temperature range from 26 to 1100 °C. The line shape of Raman spectra can be well fitted by multidamped–harmonic oscillator model. Two soft optical phonons were observed at 43.1, 52.4 cm^{-1} at room temperature. Both modes show softening approaching their corresponding phase transition temperature. It is found that damping factor γ of the lowest soft optical mode increases, while frequency of this mode decreases rapidly with temperature. Near T_c, the soft mode becomes over damped ($\gamma/\omega > 1$). The soft mode frequency related to the order parameter of this ferroelectric phase shows a non-classical behavior, and the critical exponent connected to the increase of the order parameters obtained as $\beta = 0.377$. From the relation of soft mode frequency with temperature, the ferroelectric phase transition temperature T_c was estimated to be 1058 °C.

Keywords: Soft optical phonon; Raman scattering; $Sr_2Nb_2O_7$; Phase transition

1. Introduction

$Sr_2Nb_2O_7$ (SN) is the highest T_c ferroelectric with the perovskite slab structure [1]. Low coercive field, low permittivity and high-heat resistance of this material enables its solid solutions $Sr_2Ta_xNb_{2-x}O_7$ to be used as Pb free non-volatile ferroelectric memory devices based on field effect transistors and capacitors, and optical waveguides [2–4]. Furthermore, its lead free character has received much more attention as green materials in its application.

The spontaneous polarization $P_s = 9 \times 10^{-6}$ C cm^{-2} is parallel to the *c*-axis and the coercive field is $E_c = 6$ kV at room temperature [5].The structure of SN have slabs parallel to (0 1 0), consists of an NbO_6 octahedra and Sr atoms. It was known that the octahedra distort and tilt on cooling and SN undergoes three phase transitions at 1342, 215 and −156 °C, $Cmcm \rightarrow Cmc2_1 \rightarrow Pbn2_1 \rightarrow Pb11$ [6,7]. The dynamics of phase transitions has been studied mainly by means of Raman scattering [8–11], ESR [12], and polarized far-infrared reflectivity and transmission measurements [13]. The ferroelectric soft mode was found in $b(cc)\bar{b}$ scattering geometry below $T_c = 1342$ °C. Below 215 °C another soft mode appears showing the displacive character of this normal to incommensurate phase transition. Further decreasing temperature, the soft mode coupled with another low-frequency mode, an intensity transfer occurs between the two modes. Raman, ESR and polarized far-infrared reflectivity and transmission results showed a non-classical behavior of the incommensurate order parameter with critical exponents $\beta = 0.38$, 0.34 and 0.3, respectively. As for Ba-doped SN, $(Sr_{1-x}Ba_x)_2Nb_2O_7$, the T_c decreases from 1342 °C with respect to *x* [6]. For $x = 0.32$ crystals, the low temperature ferroelectric transition temperature disappears and a new ferroic phase transition occurs at 192 °C [14].

2. Experimental

Fig. 1 shows a block diagram of a laser Raman spectroscopy setup used in the present study. Raman scattering are excited using a diode-pumped solid-state laser at a wavelength of 532 nm and a power of about 100 mW. The light beam, passing trough a narrow band pass filter, a half wavelength plate, and a polarizer, is focused onto a sample by lens L_1. Scattered light from a sample is then collected by lens L_2 using the backward scattering geometry, and

* Corresponding author. Tel.: +81-29-853-5278; fax: +81-29-853-5262.
E-mail address: anwar@ims.tsukuba.ac.jp (A. Hushur).

0272-8842/$30.00
doi:10.1016/j.ceramint.2003.12.166

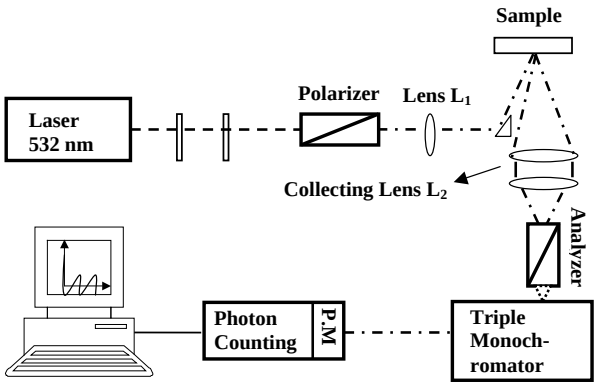

Fig. 1. The block diagram of the Raman scattering setup.

analyzed by a triple-grating spectrometer of additive dispersion (Jobin Yvon T64000). The spectral resolution was about 2 cm^{-1}. The room temperature spectra were measured in the range of 7–1000 cm^{-1}. Low frequency spectra from −100 to 200 cm^{-1} were obtained at the wide temperature range from 26 to 1100 °C. The sample was inserted into a cryostat cell (THMS600, Linkham), whose temperature stability was ±0.1 °C with ranges of −190 to 600 °C in temperature dependent Raman measurements. High temperature furnace with stability ±0.5 °C was also used for more higher temperature measurements above 600 °C.

3. Results and discussion

Space group analysis of the high temperature ferroelectric phase of SN using the structural data from the 3D X-ray diffraction [1] predicts 18 Raman active modes with the atoms in the 4*a* and 8*b* Wickoff sites, five of A_1 symmetry, four of A_2 symmetry, four of B_1 symmetry , and five of B_2 symmetry. Although this value is very close to the actual mode number in our spectra at room temperature, as can be seen in Fig. 2, mode counting in the Raman spectra of ceramic samples is very difficult due to the possible overlapping and broadening of the bands. The lowest mode was observed at 24.8 cm^{-1}. The strongest and sharpest mode was observed at 60.7 cm^{-1}. Two shoulder peaks were observed at 43.1 and 52.4 cm^{-1}. As the temperature increases, the Raman modes become broad and intense up to some temperature, after that intensity decreases (Fig. 3). However, some modes disappear completely at certain temperature which corresponds to the new ferroic phase transition, and ferroelectric to paraelectric phase transition temperature. For example, the lowest peak at 24.8 cm^{-1} at room temperature disappears above $T_r \sim 220$ °C. The mode at 52.4 cm^{-1} approaches to the mode at the 43.1 cm^{-1} in the spectra, an intensity transfer between the two modes occurs. Then the peak at 43.1 cm^{-1} tends to 20 cm^{-1} for increasing temperature and disappeared above 1051 °C. It is also observed that a significant drop in intensity of the mode at 52.4 cm^{-1}.

Light scattering intensity of Stoke shifts is given by

$$I_s(\omega) = [n(\omega) + 1] \sum \mathrm{Im}\left(\frac{S_i}{\omega_i^2 - \omega^2 + i\gamma_i\omega}\right). \quad (1)$$

where, ω_i and γ_i are the phonon frequency and the damping constant, respectively, and S_i is a constant representing the oscillator strength. The term

$$n(\omega) = \frac{1}{\exp(\hbar\omega/k_BT) - 1},$$

is so-called Bose–Einstein Factor. The first term on the right-hand side of the Eq. (1) represents the population

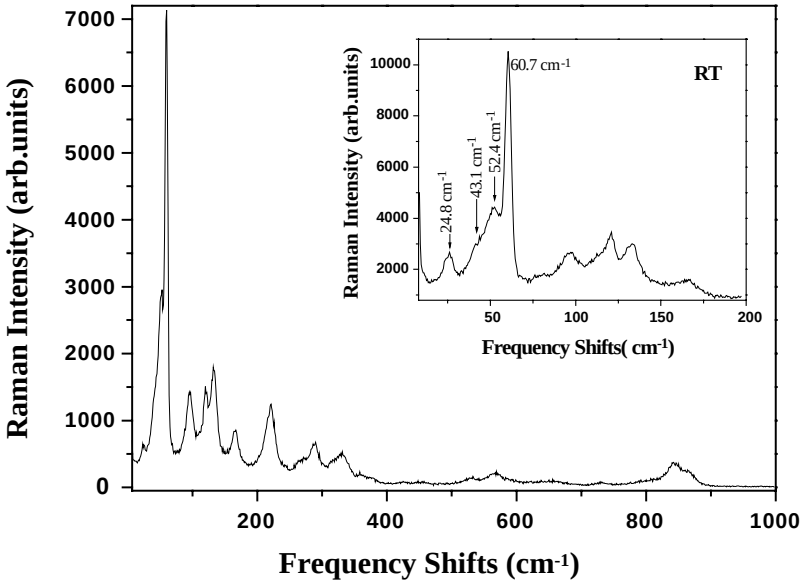

Fig. 2. Raman spectra of $Ba_{0.32}Sr_{0.68}Nb_2O_7$ at room temperature from 7 to 1000 cm^{-1}. Inset: for 7–200 cm^{-1}.

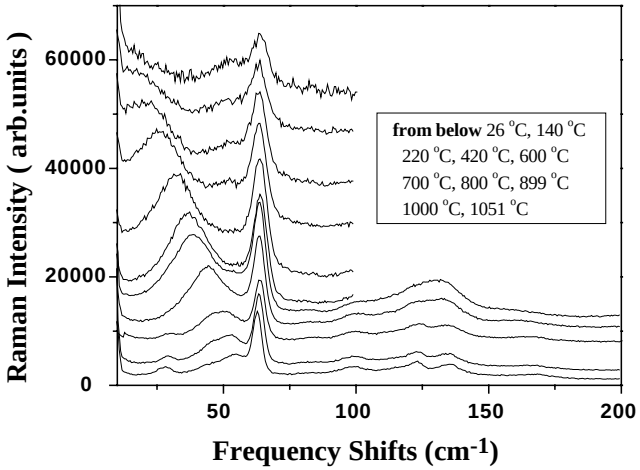

Fig. 3. Temperature dependence of Raman spectra.

density of phonons, whereas the second term is the susceptibility function for multidamped harmonic oscillator.

We fit the Raman scattering intensity using above equations. As the spectra were recorded in the same experimental conditions for all temperatures, we can thus obtain the thermal behavior of all characteristics of each phonon (frequency, damping, and strength). Some examples of the agreement which is achieved between experimental and calculated spectra are reported in Fig. 4.

Figs. 5 and 6 display the temperature dependent of the frequency and damping. In high temperature, the lowest mode exhibits a large softening with increasing temperature from the value 43.1 cm^{-1} at room temperature down to 20 cm^{-1} at 970 °C. It's damping increases so large that the soft mode becomes over damped ($\gamma/\omega > 1$). The mode at 52.4 cm^{-1} shows slight softening on approaching 220 °C from both low and high temperature sides, implies a new ferroic phase transition. It indicates that the phase

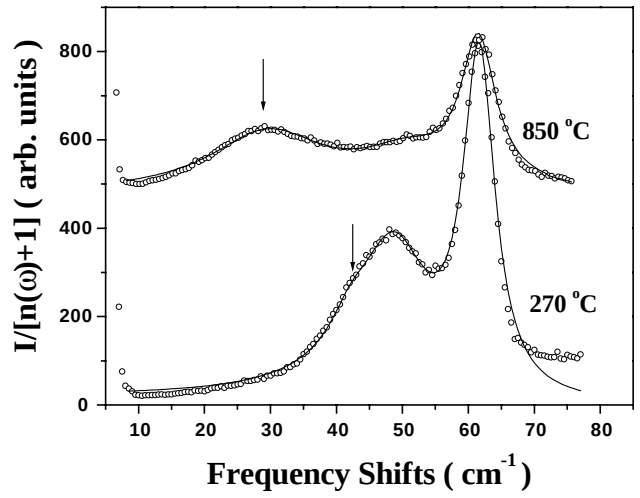

Fig. 4. Two examples of the agreement which is achieved between experimental (○) and calculated (—) spectra. Arrows indicate the low frequency soft mode.

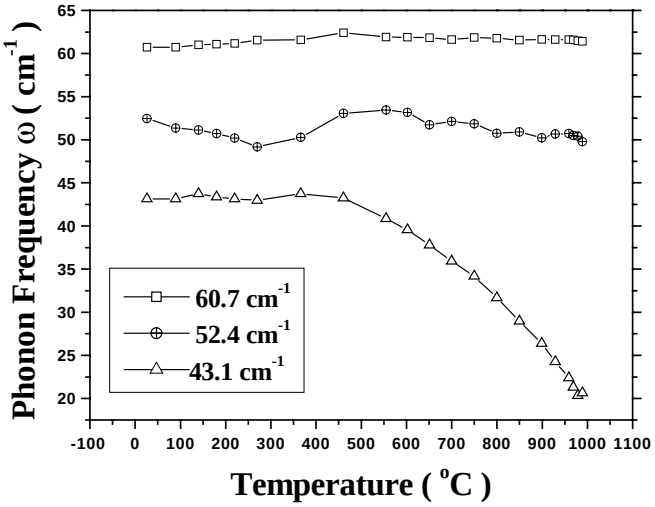

Fig. 5. Temperature dependence of the phonon frequency ω, for 43.1, 52.4 and 60.7 cm^{-1} modes at room temperature, as deduced by the fit.

transition occurs at 192 °C as observed by dielectric measurement [14].The mode at 52.4 cm^{-1} softens while the mode at 43.1 cm^{-1} shows slight hardening with the temperature approaching 220 °C and then pushes it down to lower frequencies. This implies that the ionic motions associated with the two phonon modes are transferred to each other. This makes the soft mode mechanism much more complicate.

The soft mode is $A_1(z)$ symmetry in high temperature ferroelectric phase with space group $Cmc2_1$ and responsible for the $Cmmm \rightarrow Cmc2_1$ ferroelectric phase transition. Observed soft mode frequency ω_s at room temperature for Ba-doped SN ($x = 0.32$) is much smaller than SN single crystals. According to Nanamatsu et al. [6], the ferroelectric phase transition temperature T_c of SN decreases with Ba concentration as 1077 °C at $x = 0.2$, 827 °C at $x = 0.4$.

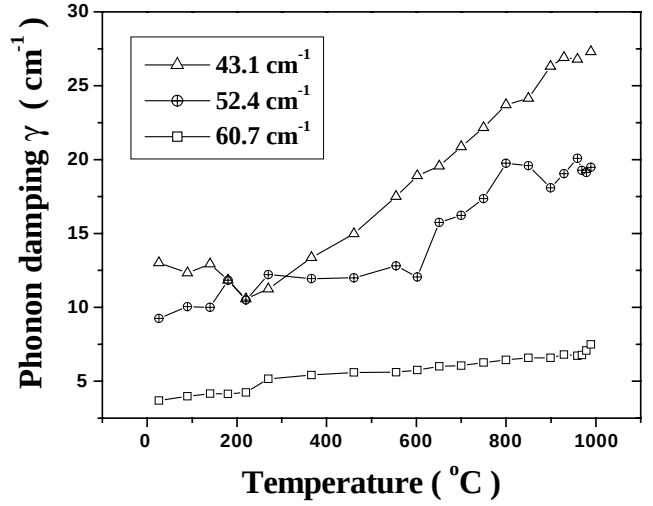

Fig. 6. Temperature dependence of the phonon damping γ, for 43.1 cm^{-1}, 52.4 and 60.7 cm^{-1} modes at room temperature, as deduced by the fit.

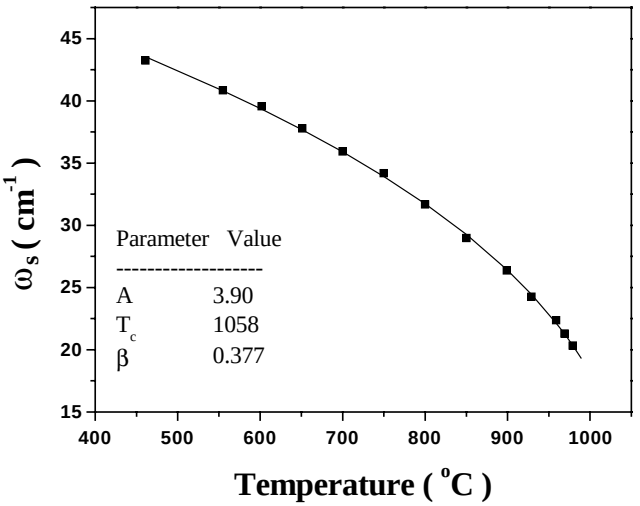

Fig. 7. The temperature dependence of the soft optical phonon frequency ω_s (■). The solid line denotes the fit $\omega_s = A(T_c - T)^{\beta}$.

Since partial replacement of Sr by Ba, whose ionic radius is larger than that of Sr, should lead to decrease of inter layer interactions, as a consequence the frequency of this soft mode can be expected to decrease with increasing Ba doping. The soft mode is probably connected with NbO_6 octahedra tiltings. Below T_c the ordered octahedra rotate within the layers, in the bc plane. The eigen-vector of the ferroelectric soft mode may be connected with these tiltings.

The quantities ω_s^2 of the soft mode for a SN single crystal have a linear relation with temperature in a wide range of about 700 °C just below T_c as $\omega_s^2 = 10.1(T_c - T)$ [11]. However, our result shows for Ba-doped SN ($x = 0.32$) different behavior. The soft mode frequency has not a linear relation but power relation with temperature. Dielectric measurements shows [6], the Curie–Weiss law is fulfilled for ε_c' with $C = 1.2 \times 10^5$ °C at $T > T_c$ and 0.42×10^5 °C at $T < T_c$. Both above and below the Curie–Weiss temperature $T_o = T_c$, which indicates the second order phase transition. We also consider the interaction between the two low frequency modes cause the line shape asymmetry, level repulsion. The decrease of soft optical phonon frequency, which is denoted as the dark squares in Fig. 7 was fitted in the $T > 366$ °C region by using $\omega_s = A(T_c - T)^{\beta}$, where A is constant. The fitted result is shown as a solid line in the same figure, and the resulting best fit parameters are 1058 ± 6 °C and 0.377 ± 0.011 for T_c and β, respectively. This indicates that the critical exponent related to the increase of the order parameter as a function of temperature in Ba-doped SN is 0.377, similar to 0.365, calculated from the Heisenberg model [15]. However, It is not clear that this feature demonstrates a non-classical behavior for the order parameter of the high temperature ferroelectric phase, because such a behavior must be expected in a narrow temperature range below T_c. It might be caused by higher-order terms in the Landau-type free energy expansion.

4. Conclusion

Raman scattering was investigated in Ba-doped $(Sr_{1-x}Ba_x)_2Nb_2O_7$ ($x = 0.32$) ceramics. Low frequency spectra from -100 to 200 cm^{-1} was obtained at the wide temperature range from 26 to 1100 °C. The ferroelectric $A_1(z)$ soft optical phonon mode, both Raman and infrared active, responsible for the $Cmcm \rightarrow Cmc2_1$ ferroelectric phase transition was observed at 43.1 cm^{-1}. An anti-crossing and energy transfer of the soft mode with another low frequency mode were observed. The line shape of Raman spectra can be well fitted by multidamped–harmonic oscillator model. It is found that damping factor γ of the soft optical mode increases, while frequency of this mode decreases rapidly with temperature. Near T_c, the soft mode becomes over damped ($\gamma/\omega > 1$). The soft mode frequency related to the order parameter of this ferroelectric phase shows a non-classical behavior, and the critical exponent connected to the increase of the order parameters obtained as $\beta = 0.377$. The behavior of the lowest mode at 24.8 cm^{-1}, and at 52.4 cm^{-1} show a new ferroic phase transition observed by dielectric measurements. We also found that the ferroelectric transition temperature T_c decreases from 1342 to 1058 °C with Ba concentration ($x = 0.32$).

Acknowledgements

This work was supported in part by the 21 Century COE program under the Japanese Ministry of Education, Culture, Sports, Science and Technology.

References

[1] N. Ishizawa, F. Marumo, T. Kawamura, M. Kimura, The crystal structure of $Sr_2Nb_2O_7$, a compound with perovskite-type slabs, Acta Cryst. B31 (1975) 1912.
[2] Y. Fujimori, N. Izumi, T. Nakamura, A. Kamisawa, Application of $Sr_2Nb_2O_7$ family ferroelectric films for ferroelectric memory field effect transistor, Jpn. J. Appl. Phys. 37 (1998) 5207.
[3] Y. Fujimori, T. Nakamura, A. Kamisawa, Properties of ferroelectric memory FET using $Sr_2(Ta, Nb)_2O_7$ thin film, Jpn. J. Appl. Phys. 38 (1999) 2285.
[4] A. Ishitani, M. Kimura, Single-crystal $Sr_2Nb_2O_7$ film optical waveguide deposited by rf sputtering, Appl. Phys. Lett. 29 (1976) 289.
[5] S. Nanamatsu, M. Kimura, K. Doi, M. Takahashi, Ferroelectric properties of $Sr_2Nb_2O_7$ single crystal, J. Phys. Soc. Jpn. 30 (1971) 300.
[6] S. Nanamatsu, M. Kimura, T. Kawamura, Crystallographic and dielectric properties of ferroelectric $A_2B_2O_7$ (A = Sr, B = Ta, Nb) crystals and their solid solutions, J. Phys. Soc. Jpn. 38 (1975) 817.
[7] K. Ohi, M. Kimura, H. Ishida, H. Kakinuma, Phase transition in $Sr_2Nb_2O_7$ at 215 °C, J. Phys. Soc. Jpn. 46 (1979) 1387.
[8] S. Kojima, M.andT. Nakamura, K. Ohi, H. Kakinuma, Optical mode softening in the incommensurate phase of $Sr_2Nb_2O_7$, Solid State Commun. 31 (1979) 755.
[9] S. Kojima, M-S. Jang, K. Ohi, T. Nakamura, Polariton dispersion and infrared active soft modes in ferroelectric $Sr_2Nb_2O_7$, J. Phys. Soc. Jpn. 50 (1981) 2787.

[10] K. Ohi, H. Omura, T. Kazumi, M. Takashige, M-S. Jang, T. Nakamura, Raman scattering from the soft phonon in $Sr_2Nb_2O_7$ for the phase transition at 117 K, J. Phys. Soc. Jpn. 51 (1982) 3745.
[11] K. Ohi, S. Kojima, Successive phase transitions and their soft modes in ferroelectric $Sr_2Nb_2O_7$, Jpn. J. Appl. Phys. 24 (1985) 817.
[12] Y. Akishige, T. Kubota, K. Ohi, ESR study of the normal-incommensurate phase transition in $Sr_2Nb_2O_7$, J. Phys. Soc. Jpn. 52 (1983) 1290.
[13] E. Buixaderas, S. Kamba, J. Petzelt, Polar phonons and far-infrared amplitudon in $Sr_2Nb_2O_7$, J. Phys: Condens. Matter 13 (2001) 2823.
[14] Y. Akishige, M. Kamata, K. Fukano, Successive phase transition of $(Sr_{1-x}Ba_x)_2Nb_2O_{7s}$, J. Kor. Phys. Soc. 42 (2003) S1187.
[15] Z. Iqbal, F.J. Owens, Vibrational Spectroscopy of Phase Transitions, Academic Press Inc., 1984.